Turkish Computational and Theoretical Chemistry

Turkish Comp Theo Chem (TC&TC)

Volume(Issue): 8(3) – Year: 2024 – Pages: 13-22

e-ISSN: 2602-3237

https://doi.org/10.33435/tcandtc.1286725

Received: 10.05.2023 *Accepted*: 13.11.2023 *Research Article*

DFT, Monte Carlo and Molecular Dynamics modeling of the Carvacrol, Camphor and Linalool /Al(111) Interaction

Fathia Laihemdi[a], Ali Barhoumi[a,b], Brahim Lizoul[c], Kamilia Mounich[a], Tariq Benabbouha[d], Mohammed Chafi[a], Abdellah Zeroual[b], Mohammed El idrissi[e, 1],

[a]LIPE, Higher School of Technology, Hassan II University, Casablanca, Morocco.
[b]Molecular Modelling and Spectroscopy Research Team, Faculty of Science, Chouaïb Doukkali University, El Jadida, Morocco.
[c]Laboratory Energy, Materials and Environment, Faculty of Sciences, Chouaïb Doukkali University, El Jadida, Morocco.
[d]Team of Thermodynamics, Surfaces and Catalysis, Faculty of Sciences, Chouaïb Doukkali University, El Jadida, Morocco.
[e]Chemical Processes and Applied Materials Team, Faculty Polydisciplinary, Sultan Moulay Slimane University, Beni-Mellal, Morocco.

Abstract: In this work, the interaction of three natural compounds: carvacrol (Inh-1), camphor (Inh-2), and linalool (Inh-3) on the Al(111) surface have been studied using DFT/B3LYP/6-31G(d,p), to understand adsorption behavior on the metal surface. The obtained results indicate a significant correlation between the inhibitory efficiency (IE%) of aluminum corrosion and the quantum chemical reactivity parameters derived from DFT. In addition, the interactions between the three natural inhibitors and the aluminum surface were studied using Monte Carlo (MC) and molecular dynamics simulations, as a result, the three molecules have strong interactions with the metal surface and thus have excellent predictive power for inhibition against metal corrosion, the three corrosion inhibitors have higher inhibitory efficiency and can be used as inhibitors to minimize the corrosion rate of the metal, therefore, the efficiency of Inh-1 is more important than the efficiency of Inh-2 and Inh-3.

Keywords: Corrosion, DFT, Dynamic Molecular, Natural Inhibitors, Carvacrol, Camphor, Linalool.

1. Introduction

The metal that is most prevalent on earth is aluminum. It makes up around 8% of the total mass of the materials on the solid surface of the Earth. It is a very common material used in industry due to its excellent mechanical properties/weight ratio and its relatively low manufacturing cost. This material is one of the main components in the aeronautical and naval transport industry [1]. Corrosion has remained a major problem in several industrial sectors, affecting the performance of various materials, including aluminum. The cost of corrosion in industrialized nations is about 3-4% of their GDP [2]. Aluminum alloys acquire their stability through the oxide hydroxide film formed on the surface. This tough, insulating film protects the metal from corrosion, by covering the entire surface; it prevents the electrons produced by the oxidation of the metal from reaching the oxide surface. This protective action cannot be provided if the oxide film is dissolved or has a defect. Exposure of aluminum to the marine environment leads to inter-granular exfoliation and cracking of the alloy. Chloride ions are characterized by their ability to penetrate the oxide film and by the formation of soluble complexes. Pitting and crevice corrosion are considered the most important types of corrosion of aluminum alloys in seawater [3, 4]. Methods used to improve the strength of aluminum alloys include corrosion inhibitors, which have

---

[1] Corresponding Authors

e-mail: m.elidrissi2018@gmail.com

proven to be a reasonable and cost-effective way to protect metals from corrosion. Generally, they are organic or inorganic compounds added at low concentrations to a corrosive environment to slow down or stop the corrosion process of metals [5]. Organic compounds can adsorb to the metal surface, thanks to heteroatoms such as oxygen, sulphur, and nitrogen. Synthetic compounds, however, are known to have excellent corrosion inhibition potential, but their toxicity to humans and the environment is proportionately high [6]. Inhibitors based on natural substances present themselves as a potential, non-toxic and biodegradable alternative. Recent research is increasingly focusing on these substances as green inhibitors [7–10]. Several bio-organic families have shown an important inhibitory effect of corrosion, such as alkaloids, phenolic compounds, and terpenes [11–13].

To understand the adsorption process as well as the corrosion inhibition mechanism of volatile products, three major compounds of different essential oils were studied as corrosion inhibitors. Carvacrol (2-Methyl-5-(propan-2-yl) phenol) is a natural monoterpene that is a major component of the essential oils of Hope Cones, Origanum vulgare, and Origanum Elongatum [14, 15]. Linalool (3,7-dimethyl-1,6-octadien-3-ol) is a terpene alcohol, the major component of the essential oil of Hyssopus officinalis [16]. Camphor, which is predominantly composed of the essential oil of Thymus vulgaris [17], whose structure of the three compounds, has been shown in figure 1.

2. Computational Method

2.1. DFT computation

Quantum methods have been widely used to understand and predict the inhibitory properties of organic inhibitors against corrosion [18, 19]. In this part, the quantum method DFT (Density Functional Theory) was used to study the adsorption mode and the nature of the molecule/surface interactions of the aluminum substrate. DFT calculations were performed to obtain the properties of the three organic molecules (carvacrol, linalool, and camphor) and to evaluate the protective character of the aluminum surface against corrosion. The effectiveness of organic inhibitors is often correlated to their electronic properties namely dipole moment (μ), electron density, HOMO and LUMO orbital energy, as well as indicators of molecular reactivity such as absolute electronegativity $(\chi = \frac{-E_{HOMO}-E_{LUMO}}{2})$[20], absolute hardness $\eta = \frac{E_{LUMO}- E_{HOMO}}{2}$ [20], nucleophilicity reactivity index $\mathbf{N = E_{HOMO(inh)} - E_{LUMO(tetracyanoethyne)}}$ [21], local indices and fraction of electrons transferred $\mathbf{\Delta N = [\chi_{Al} - \chi_{inh}]/2[\eta_{Al} + \eta_{inh}]}$ [22, 23] from the inhibitor molecule to the metal atom.

(χ_{inh}) and (η_{inh}) denote respectively the absolute electronegativity and the hardness of the inhibitor. The theoretical values of absolute electronegativity (χ_{Al}) and hardness (η_{Al}) for the aluminum atom are respectively χ_{Al} = 3.23 eV and η_{Al} = 2.77 eV [24]. The geometries of the examined molecules were optimized using the B3LYP function with the base 6-31G(d,p) [25–27]. All calculations were carried out by the program GAUSSIAN 09 [28] and visualized by GaussView (Frisch et al., 2008).[29]

2.2. Dynamics Molecular and Monte-Carlo simulations

Molecular dynamics is a very useful molecular simulation method to study all types of molecule/substrate interactions in the presence of solvent molecules (H_2O) and to identify the different adsorption modes of inhibitor molecules on the metal surface. The adsorption of the three molecules (Carvacrol, camphor, and linalool) on the aluminum surface is studied by applying Monte Carlo simulations (MC) using Materials Studio 6.0 software [30], the Al(111) surface model was selected as the aluminum crystal's more stable and compact surface [31].

The simulation box used to model the Al (111) aluminum surface has the dimensions of (34.36 Å × 34.36 Å × 51.68 Å) with periodic boundary conditions in all three directions and the inclusion of a 40 Å void layer at the C axis. The adsorption of these compounds on the Al(111) surface was simulated using the COMPASS (Condensed Phase Optimized Molecular Potentials for Atomistic Simulation Studies) force field [32], with 185 water molecules/one inhibitor molecule/6 sodium ions + 6 chloride ions. The molecular dynamics simulations were performed at 298K, the canonical NVT ensemble, with a time step of 1 fs and a simulation period of 500 ps [33, 34]. The interaction energy between the inhibitor molecules and the Al (111) interface was calculated according to the following equation [35–37].

$$\mathbf{E_{interation} = E_{total} - (E_{inhibitor} + E_{Al+H_2O})}$$

E_{total}: the total energy of the simulation system.
E_{inh}: the energy of the free inhibitor molecule.
E_{Al+H2O}: The energy of the aluminum surface and the H_2O molecules together, the binding energy being equal to the negative value of the interaction energy [36-38]:

$$E_{\mathbf{Binding}} = -E_{\mathbf{Interaction}}$$

3. Results and discussion

3.1. The relative stability of the three inhibitors

The optimized structures of the three inhibitors in the isolated state and the gas phase (figure 2), show that the equilibrium geometry of carvacrol is planar. Additionally, the structural analysis of the three inhibitors indicates that carvacrol is less energetically stable, making it the most reactive molecule due to its high total energy value in the isolated state (Table 1). This allows us to think that this molecule can form a better corrosion-inhibiting layer on the aluminium surface, unlike the other two molecules.

From the results of table 1, it can be observed that the reactivity of the three organic compounds varies in the following order: Inh-1>Inh-2>Inh-3.

3.2. Electronic properties

3.2.1. Net charges Analysis

A study of the Mulliken electron population in inhibitor molecules has been carried out, these electron populations play an important role in determining the adsorption centers of the inhibitor on the metal surface [39, 40], table 2 shows the net atomic charge values of the three inhibitors.

Table 1. DFT/B3LYP/6-31G(d,p) Total energies of carvacrol, camphor and linalool.

Inhibitors	Carvacrol	Camphor	Linalool
The total energy in (a.u)	-464.752	-465.946	-467.117

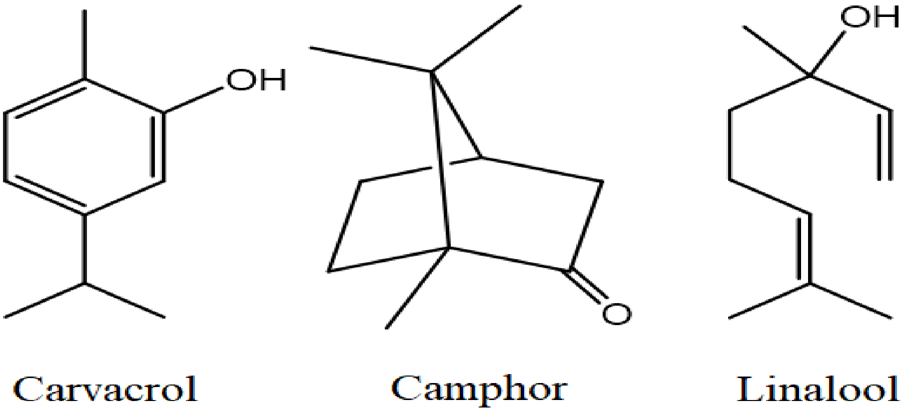

Figure 1. The chemical structures of Carvacrol, Camphor and Linalool.

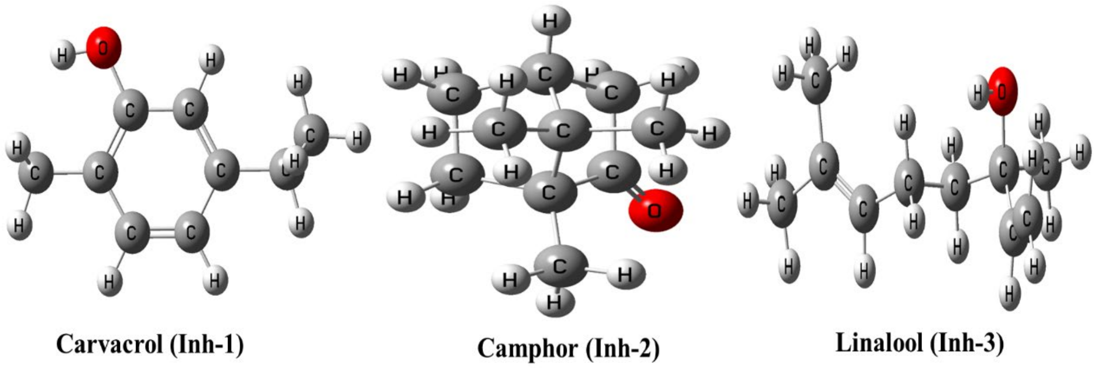

Figure 2. The most stable configuration of carvacrol, camphor, and linalool optimized by DFT/B3LYP/6-31(d,p)

Table 2. Net charges of the three organic inhibitors computed by the B3LYP/6-31G(d,p) approach.

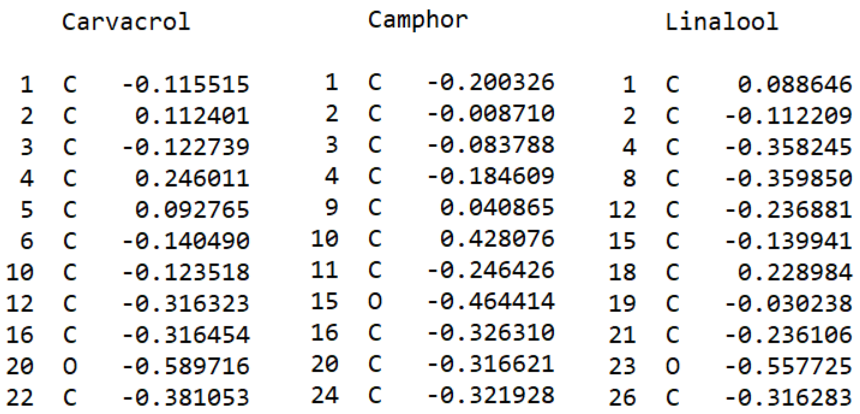

Carvacrol			Camphor			Linalool		
1	C	-0.115515	1	C	-0.200326	1	C	0.088646
2	C	0.112401	2	C	-0.008710	2	C	-0.112209
3	C	-0.122739	3	C	-0.083788	4	C	-0.358245
4	C	0.246011	4	C	-0.184609	8	C	-0.359850
5	C	0.092765	9	C	0.040865	12	C	-0.236881
6	C	-0.140490	10	C	0.428076	15	C	-0.139941
10	C	-0.123518	11	C	-0.246426	18	C	0.228984
12	C	-0.316323	15	O	-0.464414	19	C	-0.030238
16	C	-0.316454	16	C	-0.326310	21	C	-0.236106
20	O	-0.589716	20	C	-0.316621	23	O	-0.557725
22	C	-0.381053	24	C	-0.321928	26	C	-0.316283

The interaction between the metal and the inhibitor is often considered preferential on atoms characterized by extremely negative atomic charges, in the carvacrol the negative charges were localized only on carbon atoms (C1, C3, C6, C10, C12, C16, and C22) and oxygen O20, suggesting that these centers can interact with the metal surface [41, 42], this shows that oxygen is a preferred site to adsorb onto the metal surface through a donor-acceptor reaction to form a coordination bond. Table 2 also shows that the carbon atoms (C1, C2, C3, C4, C11, C16, C20, C24) and the oxygen O15 of the camphor molecule are very electron rich. Nevertheless, the two carbon atoms C9 and C10 are electron-deficient sites. It can be deduced that the oxygen O15 can give electrons to the metallic surface.

The linalool atoms (C2, C4, C8, C12, C15, C19, C21, C26, and O23) are more reactive toward an electrophilic attack, while the atoms with positive charges are more reactive toward a nucleophilic attack. In conclusion, the calculation of the net charges suggests mainly a possible electrophilic attack on the oxygen atom.

3.2.2. LUMO-HOMO Energy gap

The global and local reactivity of Camphor, linalool and carvacrol can be estimated by analyzing the HOMO and LUMO boundary molecular orbitals in the neutral and isolated states to identify the most favorable adsorption sites on the metal surface. The HOMO orbital is associated with the molecule's ability to donate electrons, while the LUMO is associated with its ability to gain electrons.

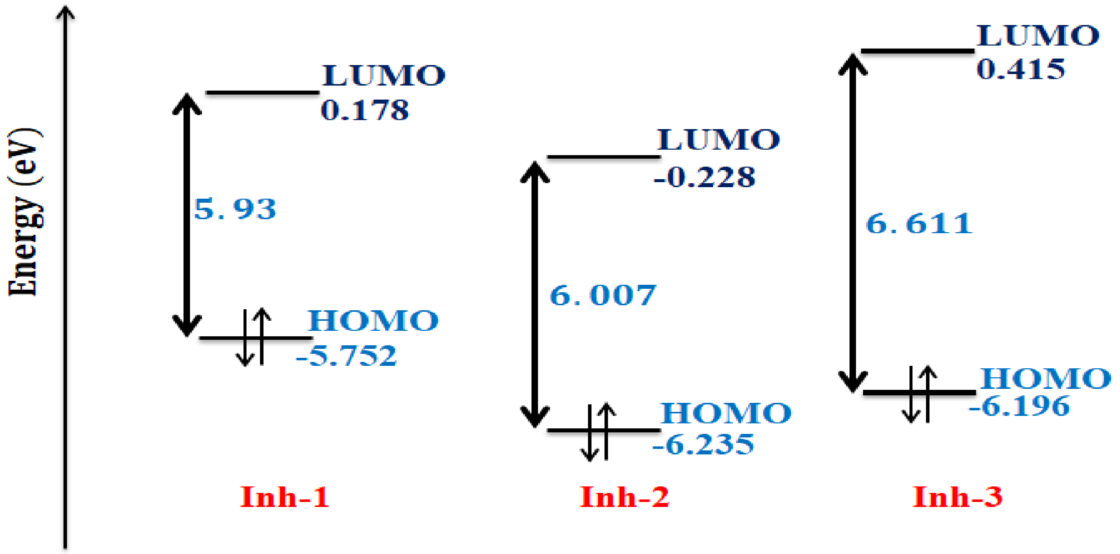

Figure 3. B3LYP/6-31G(d,p) Energy gap of the three organic inhibitors

Table 3. Quantum chemical descriptors of the three neutral inhibitors calculated by B3LYP/6-31G(d,p) (the values are given in eV).

Inhibitors	ELUMO	EHOMO	Gap	μ(Debye)	χ	η	N	ΔN
Inh-1	0.178	-5.752	5.930	1.438	2.787	2.965	3.370	0.038
Inh-2	-0.228	-6,235	6.007	2.957	3,231	3.003	2.887	-8.10^{5}
Inh-3	0.415	-6,196	6.611	1.382	2.892	3.305	2.926	0.027

Table 4. DFT/B3LYP/6-31G(d,p) Local reactivity descriptors of carvacrol.

Site K	Parr^{+}(r)	Parr^{-}(r)	f^{+}(r)	f^{-}(r)
C1	-0.1219	0.4131	-0.0028	0.1927
C2	0.3293	0.0456	0.1509	0.0888
C3	0.2738	-0.0079	0.1575	0.0161
C4	-0.0923	0.2160	-0.0261	0.1247
C5	0.3071	0.2828	0.1729	0.1090
C6	0.2946	-0.1450	0.1358	-0.0091
C10	-0.0069	-0.0016	-0.0015	-0.0374
C12	0.0132	0.0102	-0.0067	-0.0025
C16	0.0132	0.0102	-0.0071	-0.0021
O20	-0.0042	0.1805	-0.0026	0.1654
C22	-0.0299	-0.0168	-0.0008	-0.0648

Table 5. DFT/B3LYP/6-31G(d,p) Local reactivity descriptors of camphor.

Site K	Parr^{+}(r)	Parr^{-}(r)	f^{+}(r)	f^{-}(r)
C$_1$	0.0250	0.0053	-0.0040	0.0013
C$_2$	-0.0292	0.1796	-0.0182	0.0636
C$_3$	0.0029	0.0021	-0.0044	-0.0009
C$_4$	0.0007	-0.0003	-0.0107	-0.0103
C$_9$	0.0278	0.0288	0.0008	0.0140
C$_{10}$	0.5155	-0.0212	0.3343	0.0354
C$_{11}$	-0.0399	0.1374	-0.0354	0.0517
O$_{15}$	0.2777	0.5845	0.2138	0.3671
C$_{16}$	0.0040	-0.0021	-0.0188	-0.0153
C$_{20}$	0.0026	0.0199	-0.0074	-0.0055
C$_{24}$	0.0022	0.0014	-0.0170	-0.0128

Studies have shown that the effectiveness of organic inhibitors is often correlated to the LUMO-HOMO energy gap [43, 44], the lower this gap the more favorable the adsorption of the organic molecule and thus better protection of the metal surface. DFT calculations on the three inhibitors in the isolated state show that carvacrol is the most reactive molecule given its low LUMO-HOMO gap value (5.93 eV) (figure 3). The corrosion inhibition efficiency of the studied inhibitors varies in the following order: Inh-1 > Inh-2 > Inh-3.

Note also that the HOMO orbital energy (-5.752 eV) is slightly higher for carvacrol than for camphor and linalool. This confirms the stronger ability to transfer electrons from carvacrol to the metal surface. The LUMO energy (-0.228 eV) of camphor is the lowest in the isolated state, so we can think that this molecule acts as an electrophile (electron acceptor) in a system where there will be electron transfer from the substrate to the molecule.

3.2.3. Location of LUMO and HOMO orbitals

The location of the FMO boundary molecular orbitals on the atoms of the three organic inhibitors provides valuable information about the local reactivity, as shown in Figure 4 for carvacrol, the HOMO orbital is highly condensed at the carbon atoms (C$_1$ and C$_4$), and the oxygen O$_{20}$, indicates that the main interaction is between oxygen and these two carbon atoms of the inhibitor and the surface atoms of the metal when the molecule is adsorbed, it is also noted that the LUMO is distributed on the four carbon atoms C2, C3, C5, and C6 of the aromatic ring, this suggests that when the molecule adsorbs on the surface of the metal, the aromatic ring of the inhibitor molecule can get electrons. This inhibitor can adsorb to the metal surface by electron transfer, the HOMO and LUMO orbital distribution of carvacrol, camphor, and linalool are presented in figures 4, 5 and 6.

Figure 5 shows the iso-density of the HOMO orbital of camphor, according to this figure, the density of the HOMO orbital is well localized on the C2, C11, and O15 carbon atoms indicating that they are electron-rich, while the LUMO is condensed at the C10 carbon atom. This indicates that the nucleophilic attack is mainly done on the C10 atom, while, the carbon atoms (C2 and C11) and the oxygen O15 are sensitive to electrophilic attacks.

As shown in Figure 5, the HOMO orbital density is well localized on the C2, C11, and O15 carbon atoms indicating that they are electron-rich, while the LUMO is condensed at the C10 carbon atom. This indicates that the nucleophilic attack is mainly done on the C10 atom, while, the carbon atoms (C2 and C11) and the oxygen O15 are sensitive to electrophilic attacks.

From Figure 6, it can be seen that HOMO is well localized on the three carbon atoms C1, C2, and C21 indicating that it is electron-rich, while LUMO is mainly localized on the two carbon atoms C19 and C21. Therefore, the inhibitor can donate electrons via C1, C2, and C21 atoms to the unoccupied orbital to form coordination bonds, while the C19 and C21 carbons can accept electrons.

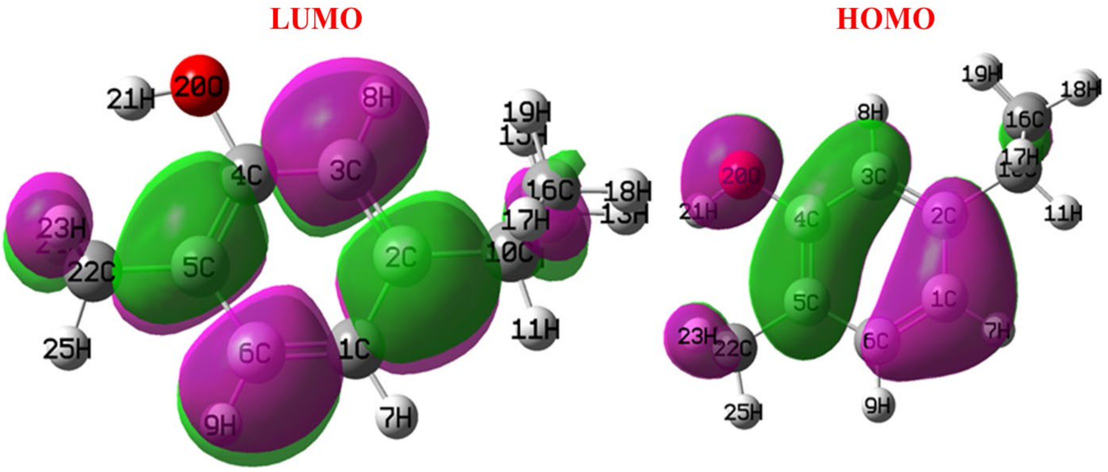

Figure 4. HOMO and LUMO boundary orbital distribution of carvacrol.

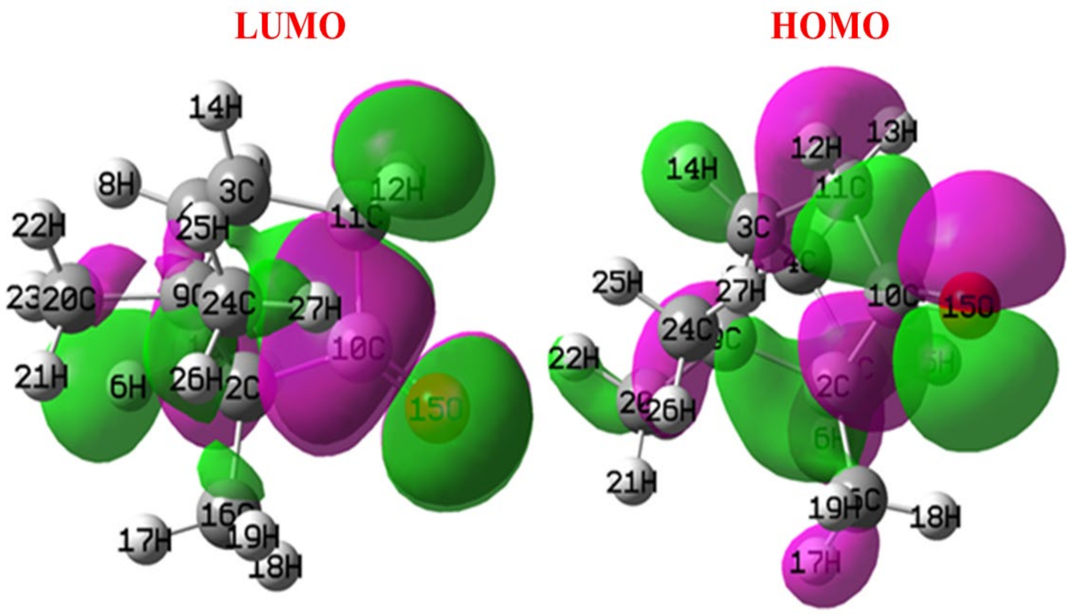

Figure 5 Iso-density of the HOMO and LUMO orbitals of camphor.

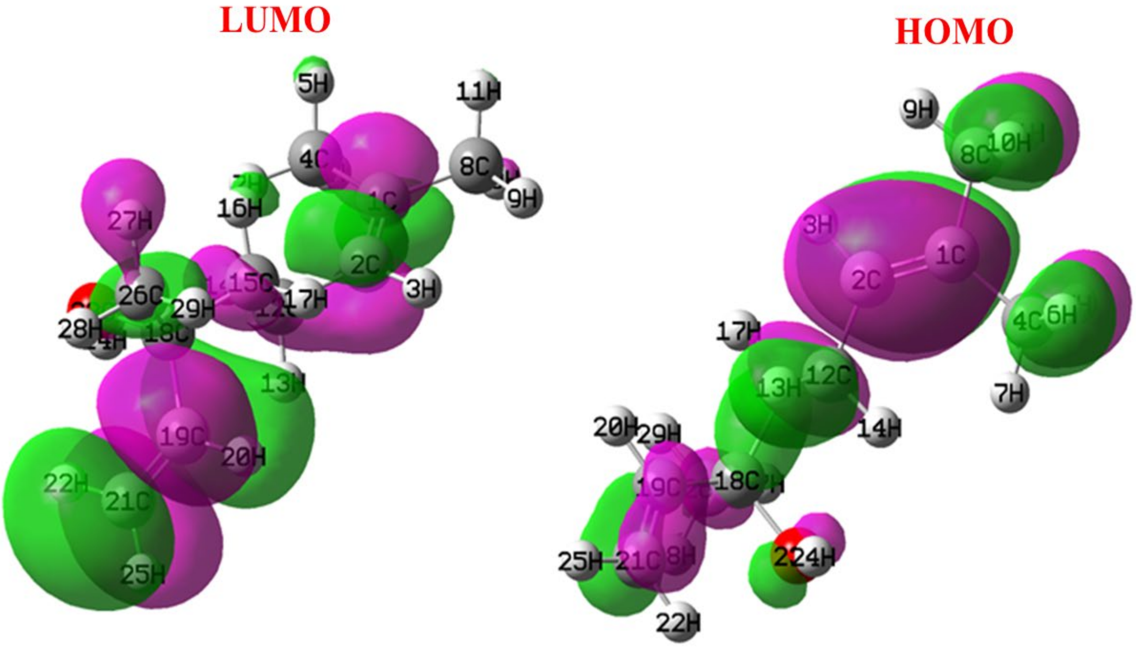

Figure 6. Iso-density of the HOMO and LUMO orbitals of linalool.

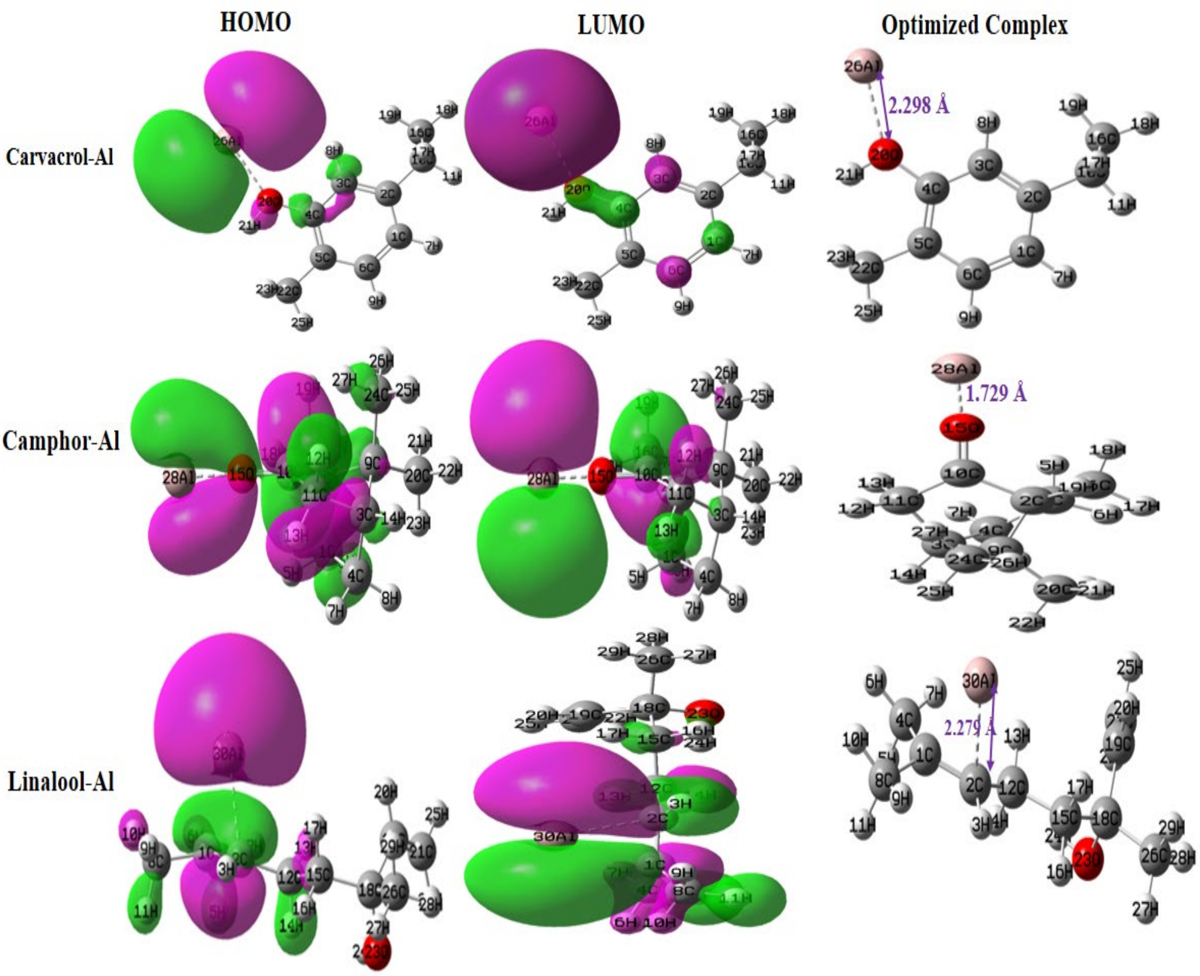

Figure 7. B3LYP/6-31G(d,p), HOMO, and LUMO iso-surface of the complex (Inhibitor-Aluminum).

Table 6. DFT/B3LYP/6-31G(d,p) Local reactivity descriptors of linalool.

Site K	$\mathbf{Parr^{+}(r)}$	$\mathbf{Parr^{-}(r)}$	$\mathbf{f^{+}(r)}$	$\mathbf{f^{-}(r)}$
C1	0.2111	0.2685	0.12896	0.17801
C2	0.1995	0.2968	0.09323	0.18277
C4	-0.0193	-0.0135	-0.01627	-0.04451
C8	-0.0188	-0.0150	-0.02133	-0.04227
C12	-0.0174	-0.0005	-0.01057	-0.03148
C15	0.0183	0.0659	0.00261	0.00173
C18	-0.0031	0.0176	-0.01067	-0.0117
C19	0.2205	0.0601	0.17587	0.02163
C21	0.3409	0.1805	0.18156	0.11962
O23	-0.0003	0.0523	0.02167	0.05218
C26	0.0053	0.0249	-0.0060	-0.00268

Table 7. Difference between the two possible LUMO/HOMO combinations for the three inhibitors and aluminum (Values in eV).

Inhibitors	$\mathbf{E_{LUMO}}$	$\mathbf{E_{HOMO}}$	$\mathbf{\lvert E_{HOMO} - E_{LUMO(Al)} \rvert}$	$\mathbf{\lvert E_{HOMO(Al)} - E_{LUMO} \rvert}$
Al	-0.433	-5.986	......	......
Inh-1	0.178	-5.752	5.319	6.164
Inh-2	-0.228	-6.235	5.802	5.698
Inh-3	0.415	-6.196	5.763	6.401

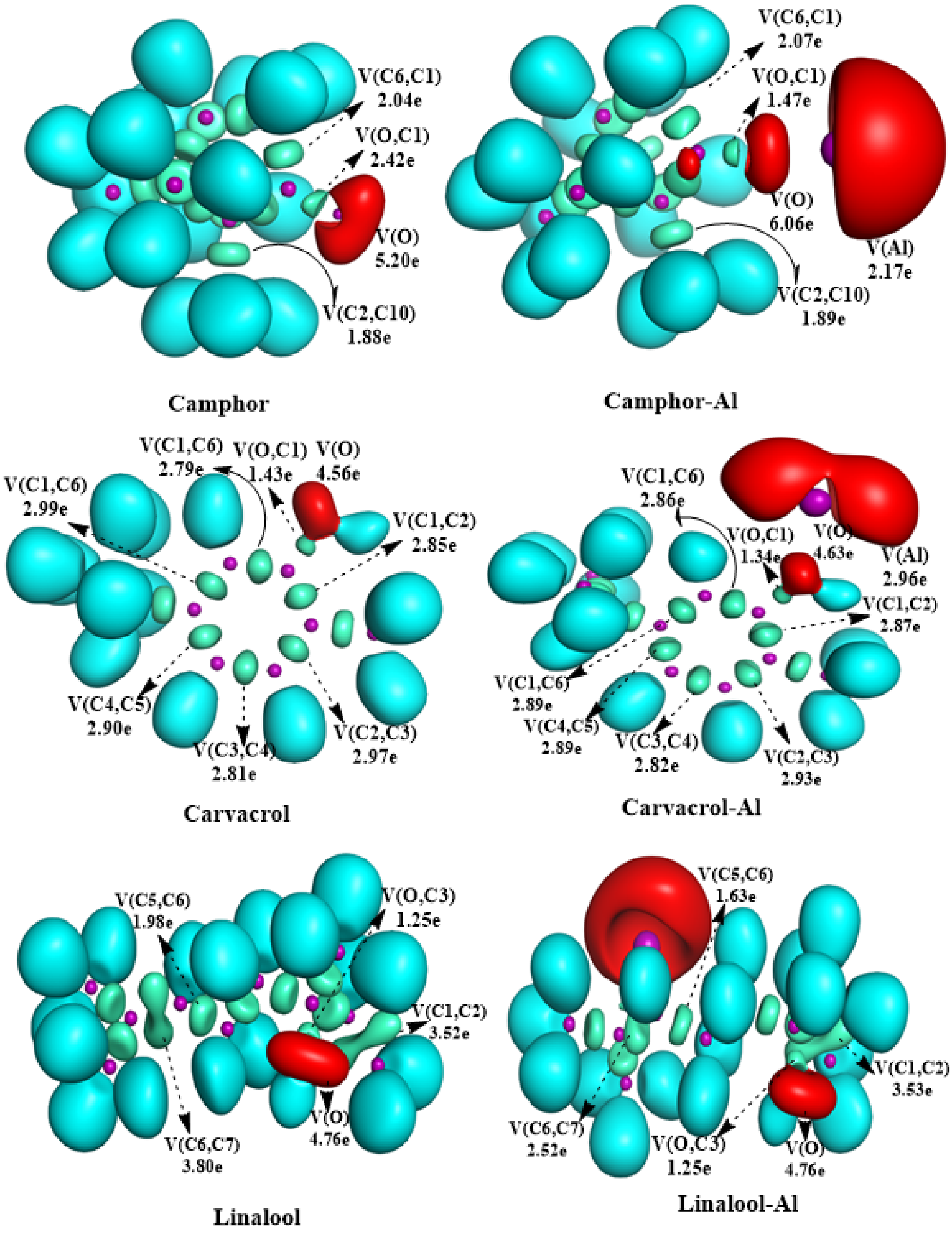

Figure 8. ELF localization domains and ELF basin attractor placements.

Table 8. Valence basin classification based on synaptic order.

Synaptic order	Nomenclature	Basin symbol
0	Asynaptic	V
1	Monosynaptic	V (Xi)
2	Disynaptic	V (Xi, Yj)
≥ 3	Polysynaptic	V (Xi, Yj, …)

3.3.3. Analysis of the global reactivity indices of carvacrol, camphor, and linalool

To assess the protective character of the three inhibitors adsorbed on the aluminum surface, several quantum chemical descriptors can be evaluated. In this section, the dipole moment (μ), electronegativity (χ), hardness (η), nucleophilicity index (N) as well as the fraction of electrons transferred (ΔN) from the inhibitor to the aluminum atom have been calculated by the B3LYP/DFT/6-31G(d,p), all these quantum chemical descriptors are presented in table 3.

According to the results presented in Table 3, carvacrol and camphor have respectively a dipole moment of (1.438 D) and (2.957 D), higher than that of linalool which is (1.382 D). Note that the higher the value of the dipole moment, the more favorable the interaction between the molecule and the aluminum surface. Thus carvacrol and camphor could interact more easily with metal surfaces than the linalool molecule. Carvacrol has a higher nucleophilicity index value (N = 3.370 eV), which suggests that this compound has a strong tendency to donate electrons to the free d orbital of the metal. This ability to donate electrons is confirmed by its low electronegativity (χ=2.787 eV). As can be seen from Table 3, camphor has a low nucleophilicity index (N=2.887 eV) while having an almost zero (ΔN) fraction, this indicates that the electron exchange is more favorable from the metal to the organic inhibitor camphor [45–48]. Therefore, the presence of carvacrol or camphor in the solution could reduce the destruction of the oxide layer and block the accessibility of the metal surface to corrosive agents.

Table 9. Binding and interaction energies between the inhibitor molecule and the Al(111) surface.

Systemes	$E_{Interaction}$ (kJ/mol)	$E_{binding}$ (kJ/mol)
Al(111) + Inh-1	-48.599	48.599
Al(111) + Inh-2	-47.736	47.736
Al(111) + Inh-3	131.053	-131.053

3.4. Reactivity local descriptors

To identify the most electrophilic (electron acceptor) and nucleophilic (electron donor) site of carvacrol, camphor, and linalool, Parr functions [49] and Fukui functions [50] are examined, these functions are more relevant for the study of selectivity.

The functions $f^{+}(r)/Parr^{+}(r)$, expresses the electrophilic character when the molecule is attacked by a nucleophilic reagent, whereas the function $f^{-}(r)/Parr^{-}(r)$ provides information about the electrophilic attack on a given site. The largest value of the $f(r)/Parr\,(r)$ function is assigned to the most reactive site [49, 50].

$f^{-}(r)/Parr^{-}(r)$ functions calculation provides the biggest value to the carbon atom (C1 and C4) and the oxygen O20, thus, these should be the most reactive sites toward electrophilic attack. Table 4, 5 and 6 reported, respectively, the local quantities for the most reactive sites of carvacrol, carvacrol, and linalool calculated by the DFT/B3LYP/6-31G(d,p) method.

The most reactive sites toward a nucleophilic attack are the atoms C2, C3, C5, and C6, indeed, the functions $f^{+}(r)/Parr^{+}(r)$ give the highest value to these carbon atoms. These reactive atoms promote the formation of stable organic layers which limits the contact between the aluminum surface and the aggressive external environment.

Table 5 also clearly shows that the C2, C11, and O15 atoms of camphor act as electron-rich (nucleophilic) centers, while the C10 carbon atom is electron-deficient. In conclusion, the main interaction is through these atoms and the metallic surface of the aluminum.

The determination of the local reactivity of linalool (Table 6) allows the identification of the different electronic transfers that take place during the linalool/ aluminium interaction. It appears that in the ground state, the two carbon atoms (C19 and C21) are the most electrophilic reaction sites, while the three carbon atoms (C1 and C2) are the most nucleophilic sites. These results predict that the atoms (C1 and C2) can transfer electrons to the aluminum surface. The inclusion of an oxygen atom and an unsaturated carbon ring, which have strong nucleophilic and electrophilic sites capable of exchanging electrons and reacting aggressively with metallic surfaces [51–53], makes carvacrol a more effective inhibitor for enhancing aluminium's corrosion resistance.

3.5. Study of inhibitor-aluminum complexes

3.5.1. Orbital aspects of the complexes

In this section, the three isolated complexes formed between an inhibitor molecule (carvacrol, camphor and linalool) and an aluminum atom were studied by the frontier molecular orbital (FMO) theory, from the analysis of the LUMO/HOMO gap calculation for the possible combinations between the three reactants and the aluminum atom, the main interaction is between the LUMO of aluminum and the HOMO of the inhibitors (Table 7), the LUMO/HOMO gaps of the formed complexes are collected in table 8 and the iso-surface of the formed complexes are presented in figure 7.

The gap corresponding to the combination $|E_{HOMO(inh)} - E_{LUMO(Al)}|$ is smaller than that corresponding to the combination $|E_{HOMO(Al)} - E_{LUMO(inh)}|$. Therefore, the inhibitors behave as nucleophiles (electron donors) during the adsorption on the substrate surface. We also notice that the gap $|E_{HOMO(carvacrol)} - E_{LUMO(Al)}|$ is smaller; this indicates the adsorption of carvacrol on the aluminum surface is very favorable.

Figure 7 shows a redistribution of the electron density of the HOMO and LUMO orbitals in the complex compared to the isolated molecule, especially on the most reactive sites of the three inhibitors. The iso-density change in the molecular orbitals of carvacrol, camphor, and linalool is a sign of coupling between the adsorbate and the substrate which also depends on the distance between the molecule and the substrate surface [54-58]. We also note that LUMO is highly condensed at the aluminum, showing that the inhibitor-aluminum complex could be the most reactive towards electron gain *via* the aluminum atom, the distances between the surface aluminum atom and the reactive atoms of the molecules involved in Al-X bond formation (X = potential active sites; i.e. O20, O15, and C2) are typical of covalent bonds.

Turkish Computational and Theoretical Chemistry

Turkish Comp Theo Chem (TC&TC)

Volume(Issue): 8(3) – Year: 2024 – Pages: 13-22

e-ISSN: 2602-3237

https://doi.org/10.33435/tcandtc.1286725

Received: 10.05.2023 ***Accepted***: 13.11.2023 *Research Article*

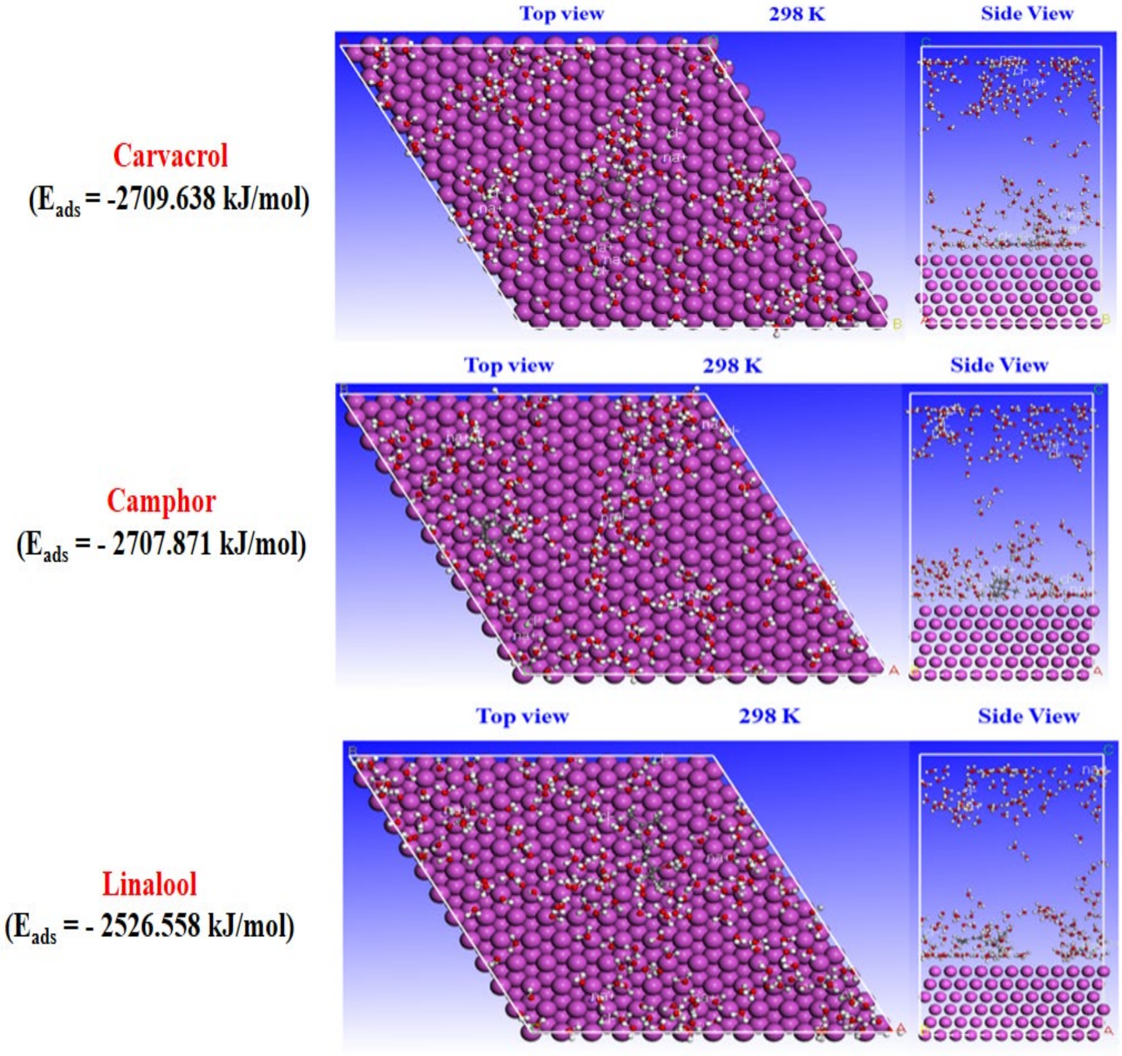

Figure 9. Top and side view of adsorption configurations of carvacrol, camphor, and linalool on Al(111) in the aqueous phase.

3.6. Topological analysis ELF of inhibitors

Due to oxidation, corrosion is an electrochemical process that elevates a metal. Rust is the oxidation of metal in the presence of air and moisture. When a refined metal naturally transforms into a more stable state, such as its oxidation, hydroxylation, or sulfuration, corrosion begins and the material deteriorates. Most metals easily oxidize because they have the propensity to lose electrons to oxygen in the air or water. In this section, we'll describe the electronic distribution at the level of the inhibitors that were researched in both isolated form and combination with the metal.

Chemical bonding has a solid foundation because of the topological analysis of ELF functions. In chemistry, it is frequently used to describe chemical bonding or reactivity. ELF attractors, or a maximum of the ELF function that identifies regions of electron pairing in space, locate areas with minimal Pauli repulsion. The nuclei-containing core basins and the valence basins are the two categories of basins that distinguish the various areas of the molecular space. If a hydrogen atom is present, a basin is protonated. A valence basin is linked to a core if the domain around the core attractor also surrounds the valence one and the two attractors are separated by a common separator. The connectivity of valence basins to a core attractor, which is determined by a synaptic order, is distributed differently. The terminology for the basins concerning synaptic order is shown in Table 8.

To determine the most basic electronic structure of the isolated inhibitors and their complexes with the metal, we first evaluated the topology of ELF. The positions of the valence basin populations, ELF localization domains, and ELF basin attractors are depicted in Figure 8, these parameters are calculated by the Topmod software [59]**.**

The topological analysis of the ELF of camphor shows the presence of two monosynaptic basins V(O) and V'(O) integrating a total population of 5.20e, a disynaptic basin V(C1, O) integrating 2.42e, and two disynaptic basins V(C6, C1) and V(C2, C10) integrating respectively 2.04e and 1.88e. The formation of a complex between the camphor and the metal changes the electronic environment around the oxygen atom. The monosynaptic basins carried by the oxygen atom take a value of six electrons V(O)=6.06e, and the value of the disynaptic basin between the carbon C1 atoms and the oxygen atom becomes V(C1, O) = 1.47e, which shows that this molecule is capable of yielding an electronic density (0.15e) to the metal, consequently camphor is capable of protecting aluminum against corrosion.

ELF topological analysis of carvacrol shows the presence of two monosynaptic basins gated by oxygen of value V(O)=4.56e, a disynaptic basin linked between the oxygen atom and the carbon atom C1, and six disynaptic basins gated by the aromatic nucleus of total value 17.37e. The formation of a complex between the oxygen atom of carvacrol and aluminum increases the value of the monosynaptic basin of oxygen and becomes V(O) = 4.63e and deprives the value of the disynaptic basin between oxygen and carbon C1, V(C1, O)=1.34e, therefore the metal is capable of accepting electrons (0.17e) from the alcohol function of carvacrol.

ELF examination of the linalool reveals the existence of two disynaptic basins linked to the C1-C2 and C6-C7 atoms with a value of V(C1, C2) = 3.53e and V(C6, C7) = 3.80e respectively, two other disynaptic basins of value V(O, C3) = 1.25e and VC5, C6)=1.98e.

In the complexation of the aluminum atom by the C6=C7 double bond of linalool, a change occurs around the double bond, the value of the basin V(C6, C7) becomes 2.52e and the value of the basin V(C5, C6) = 1.98e, while the electronic environment around the oxygen atom remains unchanged, consequently the C6=C7 double bond is capable of giving 1.28e to the metal.

3.7. Monte-Carlo simulations

Monte Carlo simulations are the use of randomized simulation techniques to model and understand chemical processes. These simulations can be used to study the dynamics of molecules, the thermodynamics of chemical systems, and reaction kinetics. Monte Carlo techniques can also be combined with other simulation methods to study complex systems such as nano-structured materials and interaction between inhibitors and metal surfaces. Top and side views of the adsorption patterns of carvacrol, camphor, and linalool on Al(111) in the aqueous phase were displayed in Figure 9.

Figure 9 indicates the adsorption energies of the three inhibitors on the Al(111) surface are all negative. Therefore, the adsorption of these organic compounds is possible and favorable. They could provide protection and form a barrier to aluminum corrosion. Moreover, we noticed that the value of adsorption energy E_{ads} which corresponds to inhibitor 1 is higher in absolute value than E_{ads} of inhibitors 2 and 3. Adsorption energy is higher in absolute value, indicating a great interaction between the inhibitor molecule and the substrate surface. Therefore, the adsorption of the inhibitor on the metal surface Al(111) with high inhibitory efficiency. Figure 9, also reveals that carvacrol is adsorbed parallel to the aluminum surface. This indicates that strong interactions occur between carvacrol and aluminum atoms. The planar adsorption mode is due to the free electrons of oxygen and the π-electrons of the aromatic ring present in carvacrol, this orientation ensures a large adsorption surface area and thus high inhibitory efficiency.

3.8. Molecular dynamics simulations

The computing interaction energies between the aluminum surface and carvacrol, camphor, and linalool are equal to - 48.599 kJ/mol, - 47.736 kJ/mol, and 131.053 kJ/mol, respectively (Table 9). The more negative the interaction energy, the more strongly spontaneous the adsorption of the inhibitors on the aluminum surface. Therefore, the binding energy of inhibitors is higher; this makes the adsorption system more stable with higher inhibitor efficiency [60]. Theoretical calculations show that the inhibitory efficiency of the studied organic compounds varies in the following order: Inh-1 > Inh-2 > Inh-3. Therefore, carvacrol can better protect the aluminum surface from corrosion. The metal surface can be protected by the formation of an inhibitory layer. These results are in good agreement with the experimental results [61, 62].

4. Conclusions

The quantum chemical descriptor values suggest that carvacrol may interact more readily with the aluminum metal surface than the camphor and linalool molecule. In addition, the study of the net charges on the atoms allowed us to show that the oxygen atom is the most negatively charged for the three inhibitor molecules. This site is classically considered a more reactive (electron donating) site. While the positive charges on the carbon atoms are likely to participate in bonding with the metal surface atoms. Local reactivity indices show that the O20, O15, and C2 sites associated with carvacrol, camphor, and linalool respectively act as electron donors during adsorption. The reactivity of the three inhibitors was discussed by calculating the energy gap between the HOMO and LUMO boundary orbitals; carvacrol would be more reactive in a system where there would be electron transfer from the molecule to the substrate.

Monte Carlo (MC) simulations show that carvacrol is positioned parallel to the metal surface reflecting the coverage of a large portion of the aluminum surface. The Monte Carlo and molecular dynamics simulations show that the organic compounds exhibit high adsorption and binding energies in absolute value during the simulation process. This indicates that the studied inhibitors are likely to adsorb onto the aluminum surface to improve the corrosion resistance, these results are in clear agreement with experimental observations.

References

[1] C. Vargel, Corrosion of Aluminium, eBook ISBN: 9780080472362, 2004.

[2] G. Koch, Cost of corrosion. Elsevier Ltd, eBook ISBN: 9780081012192, 2017

[3] R. Lumley, Fundamentals of aluminium metallurgy, 2011.

[4] A. Zaki, Elsevier Science and Technology Books, ISBN: 0750659246, 2006.

[5] R. Samiee, B. Ramezanzadeh, M. Mahdavian, E. Alibakhshi, Corrosion Inhibition Performance and Healing Ability of a Hybrid Silane Coating in the Presence of Praseodymium (III) Cations, J Electrochem Soc 165 (2018) C777–C786.

[6] VS. Hardback, Green corrosion inhibitors: Theory and Practice, Corros Eng Sci Technol 47 (2012) 249–249.

[7] X. Zuo, W. Li, W. Luo, Research of Lilium brownii leaves extract as a commendable and green inhibitor for X70 steel corrosion in hydrochloric acid, J Mol Liq 321 (2021) 114914.

[8] A. Zakeri, E. Bahmani, A. Aghdam, Plant extracts as sustainable and green corrosion inhibitors for protection of ferrous metals in corrosive media: A mini review, Corros Commun 5 (2022) 25–38.

[9] T. Benabbouha, R. Nmila, M. Siniti, The brown algae Cystoseira Baccata extract as a friendly corrosion inhibitor on carbon steel in acidic media, SN Appl Sci 2 (2020).

[10] T. Benabbouha, M. Siniti, H. El Attari, Red Algae Halopitys Incurvus Extract as a Green Corrosion Inhibitor of Carbon Steel in Hydrochloric Acid, J Bio- Tribo-Corrosion 4 (2018) 10.

[11] M. Faustin, A. Maciuk, P. Salvin, Corrosion inhibition of C38 steel by alkaloids extract of Geissospermum laeve in 1M hydrochloric acid: Electrochemical and phytochemical studies, Corros Sci 92 (2015) 287–300.

[12] M. Ben Harb, S. Abubshait, N. Etteyeb, Olive leaf extract as a green corrosion inhibitor of reinforced

concrete contaminated with seawater, Arab J Chem 13 (2020) 4846–4856.

[13] C. Verma, EE. Ebenso, MA. Quraishi, Alkaloids as green and environmental benign corrosion inhibitors : An overview. (2019) 512–528.

[14] H. Challouf, N. Souissi, M. Ben Messaouda, Origanum majorana Extracts as Mild Steel Corrosion Green Inhibitors in Aqueous Chloride Medium, J Environ Prot (Irvine, Calif) 07 (2016) 532–544.

[15] V. Vorobyova, O. Chygyrynetś, M. Skiba, Self-assembled monoterpenoid phenol as vapor phase atmospheric corrosion inhibitor of carbon steel. Int J Corros Scale Inhib 6 (2017) 485–503.

[16] G. Mazzanti, L. Battinelli, G. Salvatore, Antimicrobial properties of the linalol-rich essential oil of Hyssopos officinalis L. var decumbens (Lamiaceae). Flavour Fragr J, 13 (1998) 289–294.

[17] BH. Imelouane, JP. Amhamdi, M. Wathelet, K.Ankit, A. Khedid, Chemical Composition and Antimicrobial Activity of Essential Oil of Thyme (Thymus vulgaris) from Eastern Morocco, Int J Agric Biol 5 (2009) 205–208.

[18] G. Gece, Drugs : A review of promising novel corrosion inhibitors. 53 (2011) 3873–3898.

[19] G. Gece, The use of quantum chemical methods in corrosion inhibitor studies, Corros Sci 50 (2008) 2981–2992.

[20] RG. Parr, RG. Pearson, Absolute Hardness: Companion Parameter to Absolute Electronegativity, J Am Chem Soc 105 (1983) 7512–7516.

[21] LR. Domingo, P. Patricia, The nucleophilicity N index in organic chemistry, 7 (2011) 168–7175.

[22] I. Lukovits, E. Kálmán, F. Zucchi, Corrosion inhibitors - Correlation between electronic structure and efficiency, Corrosion 57 (2001) 3–8.

[23] VS. Sastri, JR. Perumareddi, Molecular Orbital Theoretical Studies of Some Organic Corrosion Inhibitors, Corros 53 (1997) 617–622.

[24] RG. Pearson, Absolute Electronegativity and Hardness: Application to Inorganic Chemistry, Inorg Chem 27 (1988) 734–740.

[25] AD. Becke, Density-functional exchange-energy approximation with correct asymptotic behavior, Phys Rev A 38 (1988) 3098–3100.

[26] AD. Becke, gradient correction gradient correction. 2155 (1992).

[27] C. Lee, C. Hill, N. Carolina, into a functional of the electron density f f. 37(1988)

[28] AMJ. Frisch, Gussian 09, Gaussian Inc, Wallingford CT, (2009)

[29] M. J. Frisch, A. B. Nielsm AJH, Gaussview user manual, gaussian Inc., Pittsburgh (2008)

[30] P. Taylor, RLC. Akkermans, NA. Spenley, SH. Robertson, Monte Carlo methods in Materials Studio, Mol. Simul. 39 (2013) 1153–1164

[31] F. Chiter, C. Lacaze-dufaure, H. Tang, P. Nadine, DFT studies of the bonding mechanism of 8-hydroxyquinoline and derivatives on the (111) aluminum surface. Phys Chem Chem Phys (2015).

[32] Y. Tang, X. Yang, W. Yang, A preliminary investigation of corrosion inhibition of mild steel in 0 . 5 M H 2 SO 4 by 2-amino-5- (n -pyridyl) -1 , 3 , 4-thiadiazole : Polarization , EIS and molecular dynamics simulations, Corros Sci 52 (2010) 1801–1808.

[33] H. Erramli, M. Assouag, A. Elharfi, Evaluation of corrosion inhibition performance of phosphorus polymer for carbon steel in [1 M] HCl : Computational studies (DFT , MC and MD simulations), Integr Med Res (2020) 1–13.

[34] O. Dagdag, A. Berisha, Z. Sa, DGEBA-polyaminoamide as effective anti-corrosive material for 15CDV6 steel in NaCl medium, Computational and experimental studies. 48402 (2019) 1–10.

[35] SK. Saha, A. Dutta, P. Ghosh, Adsorption and corrosion inhibition effect of schiff base molecules on the mild steel surface in 1 M HCL medium: A combined experimental and theoretical approach, Phys Chem Chem Phys 17 (2015) 5679–5690.

[36] M. Chafi, S. Byadi, A. Barhoumi, Study of copper removal by modified biomaterials using the response surface methodology, DFT Calculation, and molecular dynamic simulation, J Mol Liq 363 (2022) 119799.

[37] SK. Saha, A. Dutta, P. Ghosh, Novel Schiff-base molecules as efficient corrosion inhibitors for mild steel surface in 1 M HCl medium: Experimental and theoretical approach. Phys Chem Chem Phys 18 (2016) 17898–17911.

[38] A. Matine, A. Barhoumi, Byadi S, A. Zeroual, M. El idrissi, Corrosion inhibition performance of azelaic acid dihydrazide: a molecular dynamics and Monte Carlo simulation study, 27 (2021). J Mol Model.

[39] M. Şahin, G. Gece, F. Karcı, S. Bilgiç Experimental and theoretical study of the effect of some heterocyclic compounds on the corrosion of low carbon steel in 3.5% NaCl medium, J Appl Electrochem 38 (2008) 809–815.

[40] M. Özcan, F. Karadağ, I. Dehri Interfacial Behavior of Cysteine between Mild Steel and Sulfuric Acid as Corrosion Inhibitor, Acta Phys - Chim Sin 24 (2008) 1387–1392.

[41] IB. Obot, ZM. Gasem, Theoretical evaluation of corrosion inhibition performance of some pyrazine derivatives. Corros Sci 83 (2014) 359–366.

[42] RG. Parr, PK. Chattaraj, Principle of Maximum Hardness. J Am Chem Soc 113 (1991) 1854–1855.

[43] IB. Obot, DD. Macdonald, ZM. Gasem Density functional theory (DFT) as a powerful tool for designing new organic corrosion inhibitors: Part 1: An overview. Corros Sci 99 (2015) 1–30.

[44] MT. Majd, M. Ramezanzadeh, G. Bahlakeh, B. Ramezanzadeh Probing molecular adsorption/interactions and anti-corrosion performance of poppy extract in acidic environments. J Mol Liq 304 (2020) 112750.

[45] NO. Eddy, UJ. Ibok, EE. Ebenso, Quantum chemical study of the inhibition of the corrosion of mild steel in H2SO4 by some antibiotics. J Mol Model 15 (2009)1085–1092.

[46] VG. Maltarollo, P. Homem-De-mello, KM. Honório Theoretical study on the molecular and electronic properties of some substances used for diabetes mellitus treatment. J Mol Model 16 (2010) 799–804.

[47] MA. Quraishi, I. Ahamad, AK. Singh, N-(Piperidinomethyl)-3-[(pyridylidene)amino]isatin: A new and effective acid corrosion inhibitor for mild steel. Mater Chem Phys 112 (2008) 1035–1039.

[48] NO. Eddy, EE. Ebenso, Corrosion inhibition and adsorption properties of ethanol extract of Gongronema latifolium on mild steel in H2SO4, Pigment Resin Technol 39 (2010) 77–83.

[49] LR. Domingo, P. Pérez, JA. Sáez, Understanding the local reactivity in polar organic reactions through electrophilic and nucleophilic Parr functions, RSC Adv 3 (2013) 1486–1494.

[50] K. Fukui, Role of frontier orbitals in chemical reactions, Science (80-) 218 (1982) 747–754.

[51] AC. Balaskas, IA. Kartsonakis, LA. Tziveleka, GC. Kordas, Improvement of anti-corrosive properties of epoxy-coated AA 2024-T3 with TiO 2 nanocontainers loaded with 8-hydroxyquinoline, Prog Org Coatings 74 (2012) 418–426.

[52] AS. Fouda, AA. Al-Sarawy, FS. Ahmed, HM. El-Abbasy, Corrosion inhibition of aluminum 6063 using some pharmaceutical compounds. Prot Met Phys Chem Surfaces 45 (2009) 635–643.

[53] ML. Zheludkevich, KA. Yasakau, SK. Poznyak, MGS. Ferreira, Triazole and thiazole derivatives as corrosion inhibitors for AA2024 aluminium alloy, Corros Sci 47 (2005) 3368–3383.

[54] L. Romaner, G. Heimel, E. Zojer, Electronic structure of thiol-bonded self-assembled monolayers: Impact of coverage, Phys Rev B - Condens Matter Mater Phys 77 (2008) 1–9.

[55] A. Zeroual, M. Ríos-Gutiérrez, M. El idrissi, E.H. El Alaoui, L.R, Domingo, An MEDT study of the mechanism and selectivities of the [3+2] cycloaddition reaction of tomentosin with benzonitrile oxide, International J. of Quantum Chemistry 119 (2019) 1 9.

[56] A. Barhoumi, M. El idrissi, A. Zeroual, Theoretical study of the chemical reactivity of a class of trivalent phosphorus derivatives towards polyhaloalkanes: DFT study, J Mol Model 27 (2021) 197.

[57] S. Zouitina, A. Aboulouard, A. El Ghazali, A. Tounsi, M. El idrissi, Computational Study of New Small Molecules based Thiophene as Donor Materials for Bulk Heterojunction Photovoltaic Cells. Journal of Fluorescence 23 (2022) 553-563.

[58] M. El idrissi, A. Eşme, Y. Hakmaoui, M. Ríos-Gutiérrez, A. Ouled Aitouna, M. Salah, A. Zeroual, LR. Domingo, Divulging the Various Chemical Reactivity of Trifluoromethyl-4-vinyl-benzene as well as Methyl-4-vinyl-benzene in [3+2] Cycloaddition Reactions, Journal of Molecular Graphics and Modelling 102 (2021) 107760.

[59] L. Romaner, D. Nabok, P. Puschnig, Theoretical study of PTCDA adsorbed on the coinage metal surfaces, Ag(111), Au(111) and Cu(111), New J Phys 11 (2009).

[60] S. Noury, X. Krokidis, F. Fuster, B. Silvi, Computational tools for the electron localization function topological analysis. Comput Chem 23 (1999) 597–604.

[61] M. Messali, M. Larouj, H. Lgaz, A new schiff base derivative as an effective corrosion inhibitor for mild steel in acidic media: Experimental and computer simulations studies. J Mol Struct 1168 (2018) 39–48.

[62] K. Mounich, M. Chafi, OL. El Hachemi, A, Tizliouine, W, Wahabi Study and Conception of a Potentiostat at Competitive Prices and its Application for Assessing Aluminum Corrosion Inhibition, J Port Electrochem Soc (2023) 1185–22.